Production and Characterization of Elastic Iron (II) Tris-Bipyridine Cross-Linked PDMS Networks

by

Jacob Tyler Pawlik

Honors Thesis

Appalachian State University

Submitted to the Department of Chemistry
and The Honors College
in partial fulfillment of the requirements for the degree of

Bachelor of Science

May, 2016

Approved by:

_____
Dr. Alexander Schwab, Chemistry, Thesis Director

_____
Dr. Michael Hambourger, Chemistry, Second Reader

_____
Dr. Jennifer L. Burris, Physics & Astronomy, Third Reader

_____
Dr. Libby Puckett, Chemistry, Department Honors Director

_____
Dr. Ted Zerucha, Interim Director, The Honors College

Abstract:

A new elastomeric material made using iron (II) ions as cross-links between bipyridine-terminated polydimethylsiloxane chains (bpyPDMS) was synthesized and characterized for use as a stimuli-responsive and recyclable rubber. This material could improve the degradability of rubber waste and ease of industrial processing, also providing a visual response to material stress through color change. Characterization was performed with ^{1}H NMR spectroscopy, gel-permeation chromatography (GPC), differential scanning calorimetry (DSC), cyclic voltammetry (CV) and UV-vis spectroscopy. GPC showed clear separation of each polymer, but an unwanted UV-absorbing low molecular weight species was observed. DSC thermograms indicated suppression of PDMS crystallization by endgroups and iron (II) atoms. However, an excess of iron (II) appeared to cut bpyPDMS, shifting the crystallization peak from -33.1^{o}C to -84.2^{o}C. Titration studies suggested species of iron (II) chloride from $FeCl_2 \cdot 4H_2O$ interfered with network formation, while networks with $Fe(BF_4)_2 \cdot 6H_2O$ were 83% complete. Cyclic voltammetry showed reversible formation of the network. Future research will involve characterizing this rubber material with other techniques such as oscillating shear rheometry.

Acknowledgements/Funding Support:

I would like to thank my honors thesis committee for all their time and effort in assisting me with this paper and defense. They provided all the resources and help I needed to learn about how to write a full research paper and they encouraged me every step of the way. I especially want to thank my thesis director, Dr. Schwab, whom taught me a plethora of useful instrumental techniques, syntheses, and laboratory practices that have made me more than prepared for my future in chemistry. I felt confident and knowledgeable going into my defense presentation, and this was because of the many questions Dr. Schwab helped me answer while in the lab.

I would also like to thank all of the sources of funding for this project, including the National Science Foundation, the ACS Petroleum Research Fund, the ASU Office of Student Research and the ASU College of Arts and Sciences.

Lastly, I want to thank my family and JoAnna Michael for being supportive of my career and encouraging me throughout this project.

Table of Contents:

Table of Figures:

Table of Tables:

Table of Equations:

Introduction:

Polymers are large molecules containing many repeat subunits of covalently bound atoms such as carbon, silicon, oxygen, sulfur, or nitrogen. These molecules exhibit unique physical properties, which can be chemically tailored to form glasses instead of crystals, fold into specific shapes, be rigid or flexible, and be soluble or insoluble. Polymeric materials are typically divided into two types: thermosets and thermoplastics.

Thermoplastics are materials that become plastic, or pliable, at high temperatures and then harden when cooled. They are typically made of individual linear or branched polymer chains, and these chains associate through non-covalent intermolecular forces and physical entanglement. These intermolecular interactions include ion-dipole and van der Waals interactions, which generally become weaker at high temperatures and stronger at low temperatures. In this way, thermoplastics can be reversibly molded and are recyclable. An example of a thermoplastic polymer chain is poly(methylmethacrylate) (PMMA), whose structure is shown below in Figure 1.

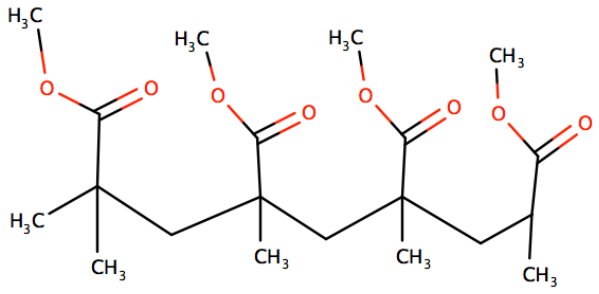

Figure 1: PMMA polymer chain comprised of four repeating subunits.

Conversely, thermosets are materials whose shape becomes set at high temperatures. This setting is due to network formation, which involves the covalent

bonding and intermolecular interactions of polymer chains or molecules. The covalent linking of these polymer subunits is called cross-linking, and the most prevalent method of cross-linking is through free-radical based chemistry.[1] A typical polymeric cross-linked network is displayed in Figure 2, which may have cross-links placed at random or systematic locations.

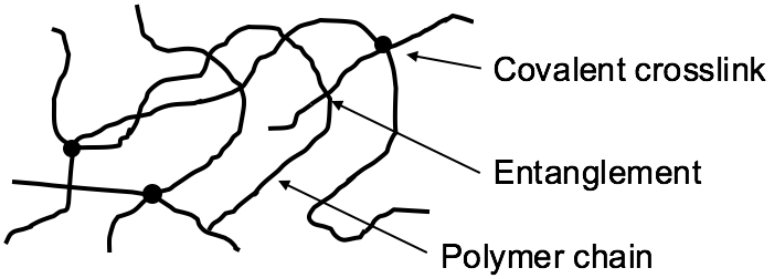

Figure 2: A thermoset network with random cross-links between polymer chains.

The stiffness of these thermoset networks can be expressed through an elastic modulus, which has the relationship below in Equation 1.[2]

$$\sigma = \frac{\rho RT}{M_c}\left(\lambda^2 - \frac{1}{\lambda}\right) \qquad Equation\ 1$$

The real stress σ is a linear function of the modulus, $\frac{\rho RT}{M_c}$. Materials with extensive cross-linking, or low molecular weights (M_c) of polymer between cross-links, are stiff and become stiffer with increasing temperature.

Thermoset materials are sometimes not composed of chains, but have only one subunit between cross-links, and these form complete networks since the maximum amount of cross-links exist. An extreme example of this type of thermoset is phenol-formaldehyde resin. These networks are very viscous and can form hard materials at

moderate temperatures. Thermosets can also have long, flexible chains that display rubber-like properties, and this type of thermoset is one example of an elastomer.

Elastomers are deformable polymer chains that are most often used to make thermoset or thermoplastic materials. In contast to PMMA, which forms a rigid glass-like material (Plexiglas), elastomers such as polydimethylsiloxane (PDMS) are flexible and act as soft adhesives and sealants. These networks are viscoelastic, meaning that they display both viscosity and elasticity under external stress. Viscosity is a measure of resistance to permanent flow in fluids while elasticity is the ability of a material to resume its normal shape after distortion. The viscoelasticity of an elastomer can change based on the composition of the polymeric chains and network interactions.

An example of a thermoset elastomeric material is styrene-butadiene rubber, which can be covalently cross-linked using dicumyl peroxide.[3] Using larger amounts of dicumyl peroxide causes the network to become stiffer. An example of a thermoplastic elastomer material is a triblock copolymer network of poly(styrene) (PS) and poly(isoprene) (PI).[4] The structure of this network involves glassy domain entrapment, or non-crystalline freezing, of the poly(styrene) end groups from the PS-PI-PS chain (Figure 3).

In addition to glassy domain entrapment, other non-covalent intermolecular interactions such as hydrogen bonding, dipole-dipole interactions, and hydrophobic interactions can act as cross-links in thermoplastic elastomer networks.[5] Since formation of the network is reversible, cross-links can also be regulated through external stimuli such as pH, salinity, temperature, and redox chemistry. In this way, multiple strategies can be used to design a uniquely behaving material.

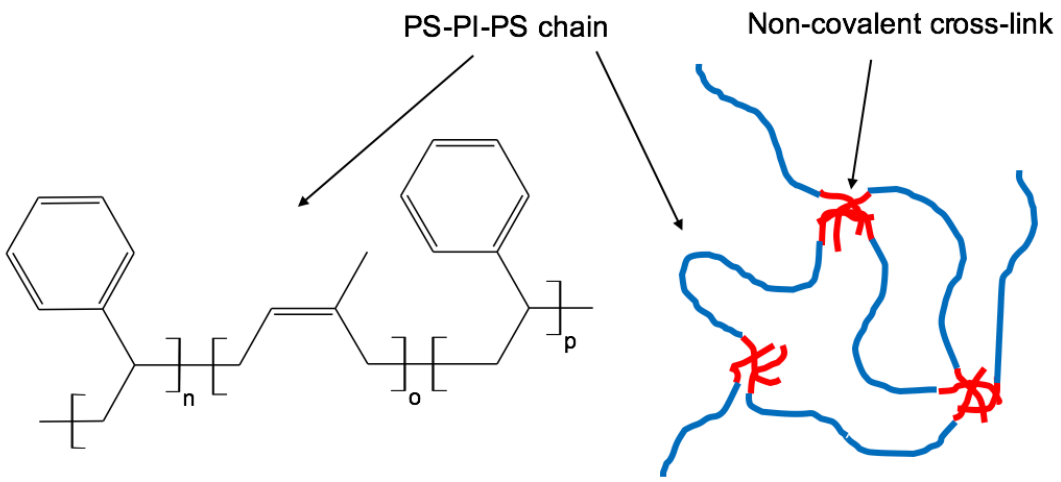

Figure 3: Thermoplastic elastomer poly(styrene)/poly(isoprene)/poly(styrene) triblock copolymer network structure.

The use of transition metal chemistry in forming cross-links is a particularly promising strategy because the interactions between metals and ligands can reach the strength of covalent bonds while being reversible. Many examples of metal-coordination cross-links have recently appeared, including gold cross-linked poly(vinyl alcohol) and FePt-nanoparticle-cross-linked siloxanes.[6] The first to perform this type of work was Belfiore, *et al.*, who used cobalt, nickel, and ruthenium (II) as cross-linking agents for chains of poly(4-vinylpyridine).[7] They demonstrated that this type of cross-linking significantly enhances the glass transition temperature, improving thermal stability. This cross-linking strategy has the greatest potential in designing recyclable rubber materials since this added reinforcement can raise the elastic modulus high enough to compete with that of conventional rubbers.

There are multiple cross-linking patterns that can be employed to control the structural properties of networks. Two common ways are shown below in Figure 4, where linking groups are either attached along a polymer chain or at the ends.

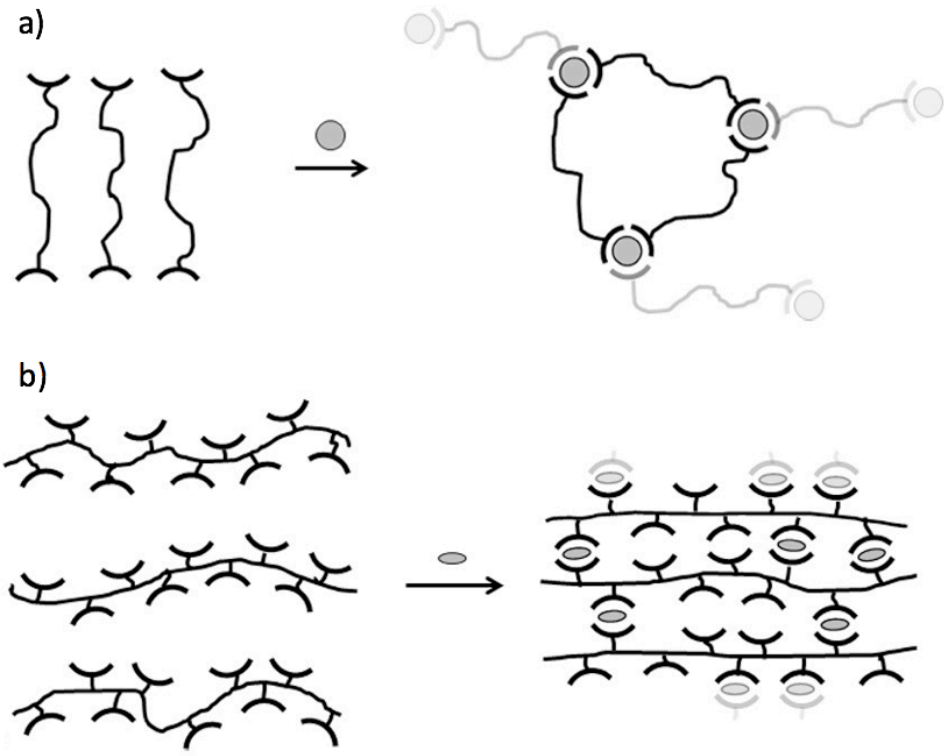

Figure 4: a) Cross-linkers (semi-circles) attached along the polymer chain. b) Cross-linkers attached at end of polymer chain.

Configuration (a) involves the placement of linking groups at the ends of polymer chains, which associate to cross-linking agents (gray circles) and form webs of networked material. In the above case (Figure 4), this web is composed of triangle-shaped patterns since the cross-linking agents associate with three linking groups. Configuration (b) involves the random placement of linking groups along polymer chains, forming stack-like structures when cross-linking agents are attached. This configuration is less useful

than configuration (a) because the ratio of linking groups to cross-linking agent cannot be controlled and the structure of the network is harder to functionalize. With configuration (a), the endgroups can be easily functionalized and the molecular weight between cross-links is often known.

Modern thermoplastic elastomers are not replacing non-recyclable thermoset elastomers because these networks cannot reach the stiffness and durability provided by the covalent cross-links in rubber materials. The problem with thermoset networks is they are difficult to process and are permanent once formed. Easier manufacturing can be achieved with thermoplastic elastomers because they can be re-shaped through injection molding and are able to be tuned for specific properties.

It is proposed that the polymer polydimethylsiloxane (PDMS) with bipyridine end groups (configuration (a), Figure 4) can be cross-linked into an organized network through coordination with iron (II) atoms in a tris-bipyridine fashion. Theoretically, this network will act as a thermoplastic elastomer with reversible iron (II) cross-links to produce a tangible, rubbery material with a comparable elastic modulus to modern covalently cross-linked rubbers. This network would be reversibly produced by oxidation/reduction of iron (II) to iron (III), where the iron (III) atom does not coordinate to bipyridine and will not participate in network formation. This material would be useful as a stimuli-responsive rubber, where the stimulus is the oxidation/reduction of iron. Since electrolytic redox reactions are simple, this material can be easily recycled and act as an environmentally-friendly rubber. The tris-bipyridine iron (II) complex also exhibits a red coloration, which is a useful indicator in determining the amount of complexation. If the material is damaged, it may display discoloration.

Figure 5 shows the structure of this proposed network. Using configuration (a) (Figure 4) for building the network allows for greater elasticity and a 3:1 coordination of bipyridine to iron (II) atoms.

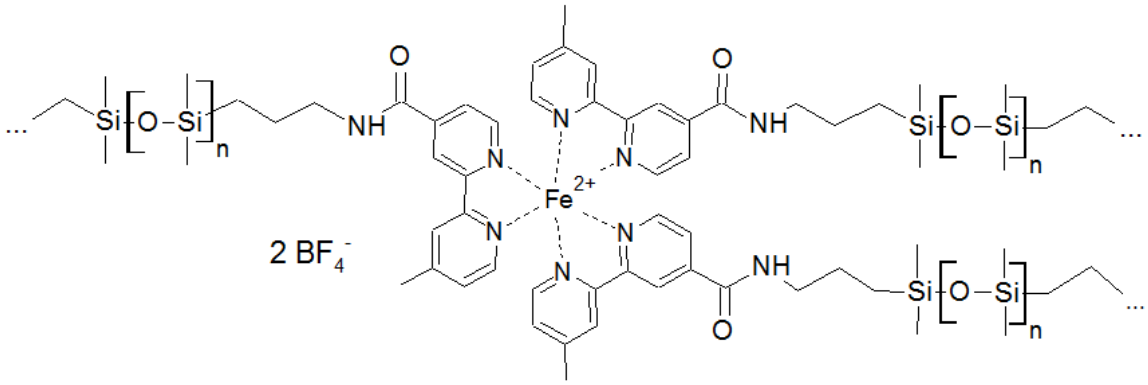

Figure 5: The cross-link structure in the iron (II) tris-bipyridine PDMS network.

In this report, the PDMS chain length was varied to explore the effect on the elasticity of the material. The longer the chain, the more flexible and elastic this network becomes according to the modulus term in Equation 1. Four viscosities of PDMS were used: 50 cSt, 100 cSt, 1000 cSt, and 5000 cSt. The unit cSt is equivalent to mm^2/s, and describes the diffusivity of momentum, typically of a polymer. The molecular weight can be expressed as a viscosity since they are linearly related; a higher molecular weight polymer with a longer chain will experience more physical entanglement and be more viscous.

The synthesis of this cross-linked network, shown in Figure 6, involves the addition of monocarboxy bipyridine (mcbpy) to amine-terminated PDMS (NH_2-PDMS-NH_2 or simply NH_2PDMS) through nucleophilic attack, then incorporation of either $FeCl_2 \cdot 4H_2O$ or $Fe(BF_4)_2 \cdot 6H_2O$ in deoxygenated THF to produce the iron (II) tris-bipyridine PDMS network.

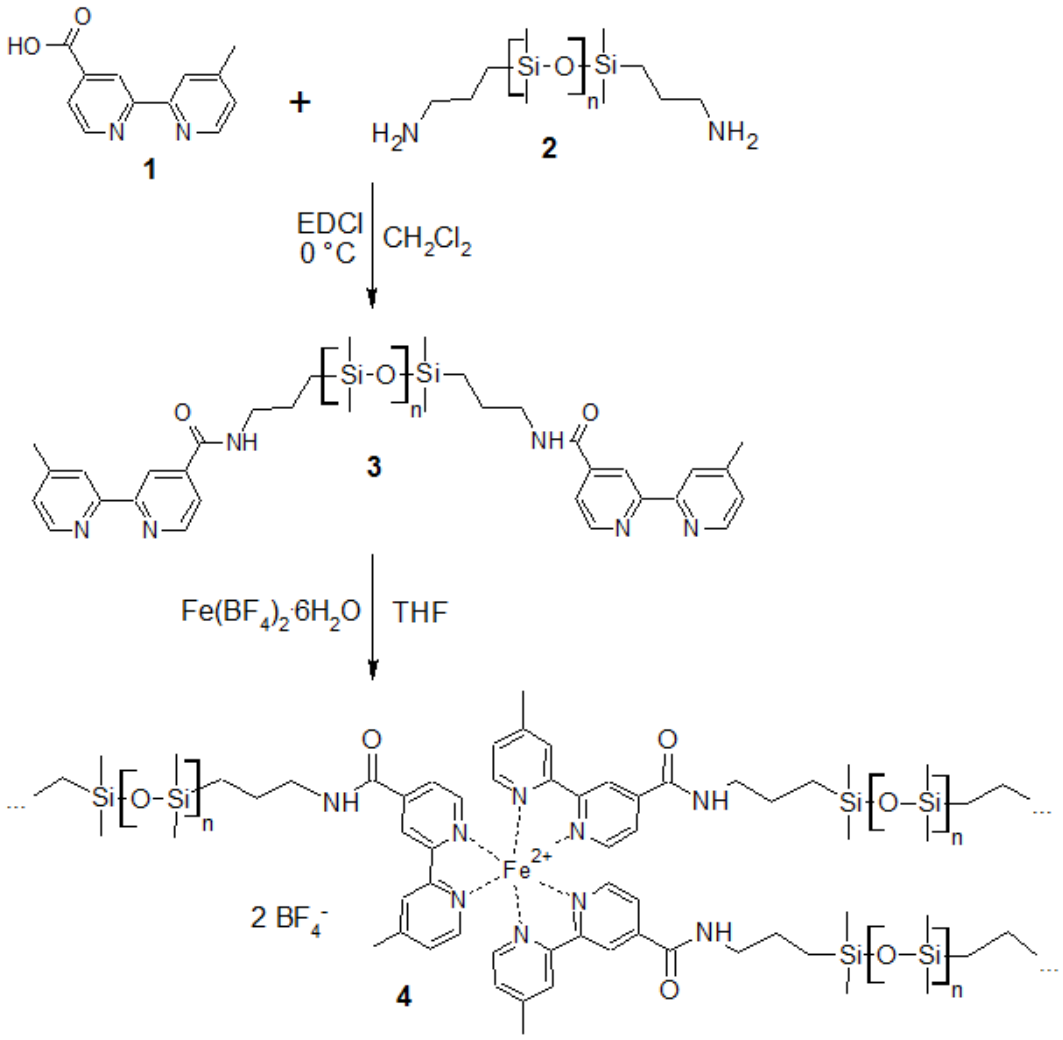

Figure 6: Synthesis of cross-linked iron (II) tris-bipyridine PDMS.

Studies have shown that supramolecular gels with some configuration of non-covalent cross-links can be a useful stimuli-responsive and self-healing materials.[8] The only evidence of elastomeric metal-coordination polymer networks is from Rowan, *et al.* using polytetrahydrofuran and polyethylene-co-butylene, so there is much to be explored within this subject area.[9] Upon careful design and improvement, a recyclable elastomer network could compare elastically to covalent thermoset rubbers, but improve their stimuli-responsive behavior and environmental impact. In this thesis, the characterization

and synthesis of the iron (II) tris(bipyridine) PDMS network and components will be addressed along with its chemical properties.

Experimental:

A) Synthesis of mcbpy

4-methyl-2,2'-bipyridine-4'-carboxylic acid (mcbpy, Figure 6-1) was synthesized according to McCafferty, D.G., *et al*.[10] A suspension of SeO_2 (3.0754 g, 1.2 eq.) and 4,4'-dimethyl-2,2'-bipyridine (4.2585 g, 1 eq.) in 1,4-dioxane (250 mL) was refluxed for 24 hours while stirring, filtered hot through Celite and then the solvent was removed at reduced pressure. The yellow solid was suspended in 95% ethanol (150 mL), then a solution of $AgNO_3$ (4.3132 g, 1.1 eq.) in water (40 mL) was added and Ag_2O was formed after adding 1M NaOH (100 mL) dropwise over 20 minutes. The black solution was subjected to rotary evaporation after stirring for 15 hours then Ag_2O and elemental silver were removed by filtration through a glass-frit. After washing with 1.3 M NaOH (2X 30 mL) and water (1X 30 mL), dichloromethane (4X 100 mL) was used to extract unreacted bipyridine. The solution was adjusted to pH 3.5 with 1:1 (v/v) 4.0 N HCl: 17.0 M acetic acid, then refrigerated overnight. The resulting white solid was subjected to Soxhlet extraction in acetone for 72 hours, which slowly separated mcbpy from 4,4'-dicarboxy-2,2'-bipyridine. The solvent was removed at low pressure, resulting in mcbpy (0.8429 g, 17.04%).

B) Synthesis of bpyPDMS

Approximately 2.2 eq. of mcbpy (79.8 mg) was added to NH_2-PDMS (0.5064 g, 1 eq.) (Figure 6-2) (VWR, viscosities 50 cSt, 100 cSt, 1000 cSt, and 5000 cSt) dissolved in CH_2Cl_2 (20 mL) at 0^oC and stirred. Next, 2.2 eq. of N-(3-dimethylaminopropyl)-N'-

ethylcarbodiimide hydrochloride (EDCI) (71.4 mg) was added drop-wise to the solution and stirred for 24 hours at 0 ^{o}C. After an aqueous workup in 80 mL of dichloromethane with deionized water (2X 160 mL), saturated bicarbonate solution (1X 160 mL), and brine (1X 160 mL), bpy-PDMS (Figure 6-3) (0.3264 g, 95%) resulted. The four viscosities of bpyPDMS indicated previously were all synthesized and analyzed.

C) Instrumental techniques

I. ^{1}H NMR spectroscopy

The experiment was performed with a 400 MHz Bruker AVANCE III equipped with an autosampler. Samples of bpyPDMS and NH_2PDMS were prepared by adding 7.5 mg to 750 μL of $CDCl_3$ in an ^{1}H NMR tube, then analyzed with a relaxation time T1 of 2.5 seconds. Samples of mcbpy were prepared in a similar manner, except the solvent was D_2O in trimethylsiloxane (TMS) (1.0 mL) mixed with NaOD (30 μL).

The following chemical shifts were obtained:

mcbpy δ 2.4 ppm (s, 3H, -CH_3) δ 4.9 ppm (s, 2H or 1H, DHO or H_2O) δ 7.3 ppm (d, 1H, bpy-H) δ 7.5 ppm (s, 1H, bpy-H) δ 7.7 ppm (d, 1H, bpy-H) δ 8.1 ppm (s, 1H, bpy-H) δ 8.4 ppm (d, 1H, bpy-H) δ 8.6 ppm (d, 1H, bpy-H).

NH_2PDMS δ 0.1 ppm (m, many H, -Si-CH_3) δ 0.5 ppm (t, 2H, propyl -CH_2-) δ 1.5 ppm (q, 2H, propyl -CH_2-) δ 2.6 ppm (t, 2H, propyl -CH_2-) δ 7.3 ppm (s, 1H, $CHCl_3$).

bpyPDMS δ 0.1 ppm (m, many H, -Si-CH_3) δ 0.6 ppm (t, 2H, propyl -CH_2-) δ 1.6 ppm (q, 2H, propyl -CH_2-) δ 3.5 ppm (t, 2H, propyl -CH_2-) δ 7.2 ppm (d, 1H, bpy-H) δ 7.8 ppm (d, 1H, bpy-H) δ 8.3 ppm (s, 1H, bpy-H) δ 8.5 ppm (d, 1H, bpy-H) δ 8.6 ppm (s, 1H, bpy-H) δ 8.7 ppm (d, 1H, bpy-H).

The molecular weight of each viscosity of NH_2PDMS (50 cSt, 100 cSt, 1000 cSt, 5000 cSt) was obtained by integrating the ^{1}H NMR and determining the ratio of siloxane backbone CH_3 (δ 0.1 ppm) to terminal CH_2 groups (δ 3.5 ppm), multiplying by six since there are three CH_2 groups on either end of NH_2PDMS, then dividing by six (6 H per siloxyl -$Si(CH_3)_2O$- subunit) and multiplying by 74.09 g/mol, the molecular weight of a siloxyl group. The uncertainty in this measurement was determined by calculating the difference in using either of the two CH_2 peaks to obtain the molecular weight.

II. Gel-permeation chromatography (GPC)

The GPC instrument was equipped with a 250 mm X-Stream H_2O mixed-bed (Cat. No: 33025) (10 mm diameter) column with Hitachi L-7100 pump, Eppendorf TC-50 oven, a Perkin-Elmer LC-95 UV-Vis spectrophotometer at 295 nm, and an Alltech Varex MKIII evaporative light-scattering detector (ELSD). The eluent used was a 3% solution of n-butylamine: toluene, and the flow rate was 1.000 mL/min. A 1.0 wt% solution (10 mg in 1.0 g) of NH_2PDMS or bpyPDMS in toluene was syringe-filtered (0.45 μm PTFE) and injected into the GPC column (200 μL). The column oven was set to 50 ^{o}C, and signals from the UV-vis spectrophotometer and ELSD were monitored. Both NH_2PDMS and bpyPDMS eluted around 700-900 seconds. In one experiment, 50 cSt and 5000 cSt NH_2PDMS (2 g) was heated in an evacuated oven overnight at 200 ^{o}C, then analyzed with GPC. This same NH_2PDMS was used to make 50 cSt and 5000 cSt bpyPDMS, and this was also analyzed with GPC.

III. Differential scanning calorimetry (DSC)

The instrument used for DSC was a Netzsch DSC 200 F3 Maia with 25 μL aluminum crucibles and lids, equipped with a robotic arm and self-loading system.

Helium gas flowed at 20 mL/min around the oven. It was calibrated using adamantine (onset melting point: -64.4 ^{o}C), bismuth (271.1 ^{o}C), cesium chloride (476.2 ^{o}C), indium (156.3 ^{o}C), tin (231.7 ^{o}C), and zinc (419.1 ^{o}C). Each sample was analyzed using the following program: -150 ^{o}C, equilibrate (equil.) for 15 min, 50 ^{o}C, equil., 25 ^{o}C, equil. The heating ramp was 10 ^{o}C/min. This sequence was performed for two heatings per sample and required the use of liquid nitrogen.

A mass of 50 mg of sample (NH_2PDMS, CH_3PDMS, bpyPDMS) was added to a pre-weighed DSC plate with a glass pipet and sealed with a press. A hole was poked in the top edge of the pan so that the pressure was constant. A reference and blank with known masses were also used within the sequence. Signals including glass transitions, melting, and crystallization peaks were analyzed by peak area and onset temperatures.

Samples of bpyPDMS, CH_3PDMS, and NH_2PDMS with $Fe(BF_4)_2 \cdot 6H_2O$ were made in a similar manner. Masses of 0.0356 g 50 cSt CH_3PDMS and 0.0030 g $Fe(BF_4)_2 \cdot 6H_2O$ were combined in a round bottom flask to produce a CH_3: Fe ratio of 2.83:1. For 50 cSt NH_2PDMS, 0.0380 g of the polymer and 0.0024 g $Fe(BF_4)_2 \cdot 6H_2O$ were combined, resulting in a 2.70:1 ratio. The following volumes of an iron solution were added to ~0.02 g 50 cSt bpyPDMS in a round bottom flask: 0.17 mL (6.26E-5 g $Fe(BF_4)_2 \cdot 6H_2O$, 77.7:1 bpy:Fe ratio), 0.56 mL (3.27E-4 g, 15.4:1 ratio), 1.7 mL (1.92E-3 g, 2.64:1 ratio), and 3.4 mL (3.76E-3 g, 1.02:1 ratio). The networked gel was then analyzed.

IV. Cyclic voltammetry (CV)

A drop of bpyPDMS with $Fe(BF_4)_2$ solution in THF with a bpy: iron (II) ratio of 3:1 was placed on a flat Pt electrode and the THF was allowed to evaporate. The rubber

coated electrode was then placed in a 0.1 M tetrabutylammonium hexafluorophosphate solution in acetonitrile and connected to a potentiostat (Pine Instruments, WaveNow potentiostat) as the working electrode. A Pt wire was used as the counter electrode and a AgCl coated Ag wire as the reference electrode. At the completion of a measurement, the potential of the pseudoreference electrode was corrected to the saturated calomel electrode (SCE) scale using ferrocene as an internal standard.[11]

D) Titrations of bpyPDMS

Spectra of the iron (II) tris(bipyridine) PDMS network were obtained using a Shimadzu UV-2600 spectrophotometer in absorbance mode from 275 nm to 800 nm, with a slit width of 0.1 nm at medium speed. Solutions of $Fe(BF_4)_2 \cdot 6H_2O$ (0.0193 g, 3 eq.) in THF (50 mL) and 50 cSt bpyPDMS (0.0101 g, 2 eq.) in a quartz cuvette with THF (5.37 mL) were prepared airlessly, then spectra were obtained of the cuvette after each of ten 50 μL additions of the iron (II) solution, which produced red coloration. The purity of the THF was as received. The absorbance at 540 nm was plotted versus iron (II) concentration to determine the endpoint of network formation, or where additions no longer increased absorbance.

E) Thin-film production

Thin films (sandwiches) of the iron (II) tris(bipyridine) PDMS network were produced by mixing a solution of 50 cSt bpyPDMS (0.0249 g) in THF (850 μL) with $Fe(BF_4)_2 \cdot 6H_2O$ (0.0115 g) in THF (5 mL) through a syringe under nitrogen gas, then pipetting the resulting red solution onto a glass slide periodically in small amounts while THF evaporated. Another slide was placed on top with 200 μm aluminum foil spacers at

each corner and pressed with binder clips. This fixture was placed in a 110 ^{o}C oven for two hours, then cooled. The film was red in color and used for UV-vis spectroscopy.

F) Production of physical rubbery discs

A solution of cross-linked network, prepared as in section E, was deposited in a 1 cm internal diameter Teflon cylinder fixed to a glass slide, then left to dry. Material which was adhesive towards the walls of the tube was washed with THF and the tube was left to dry again.

Results/Discussion:

A. ^{1}H NMR Spectroscopy

^{1}H NMR spectroscopy is used to detect hydrogen atoms within a molecule, which may help to confirm or elucidate structural properties of the substance. A magnetic field is used to align the spins of hydrogen atoms in the *z*-axis, then this vector is forced into the *xy*-plane and allowed to relax back to the original state. To oppose the external field, hydrogen atoms generate a secondary field that shields the nucleus, and this has a characteristic resonance frequency which is dependent on absorption of radiowaves. This shielding is altered by neighboring atoms, and this is expressed quantitatively through chemical shift (ppm). Splitting of ^{1}H NMR signals indicates neighboring hydrogens in an "$n + 1$" fashion, where n is the number of split signals.

The ^{1}H NMR spectra obtained for 50 cSt bpyPDMS, mcbpy, and 50 cSt NH_2PDMS are shown in Figure 7 below.

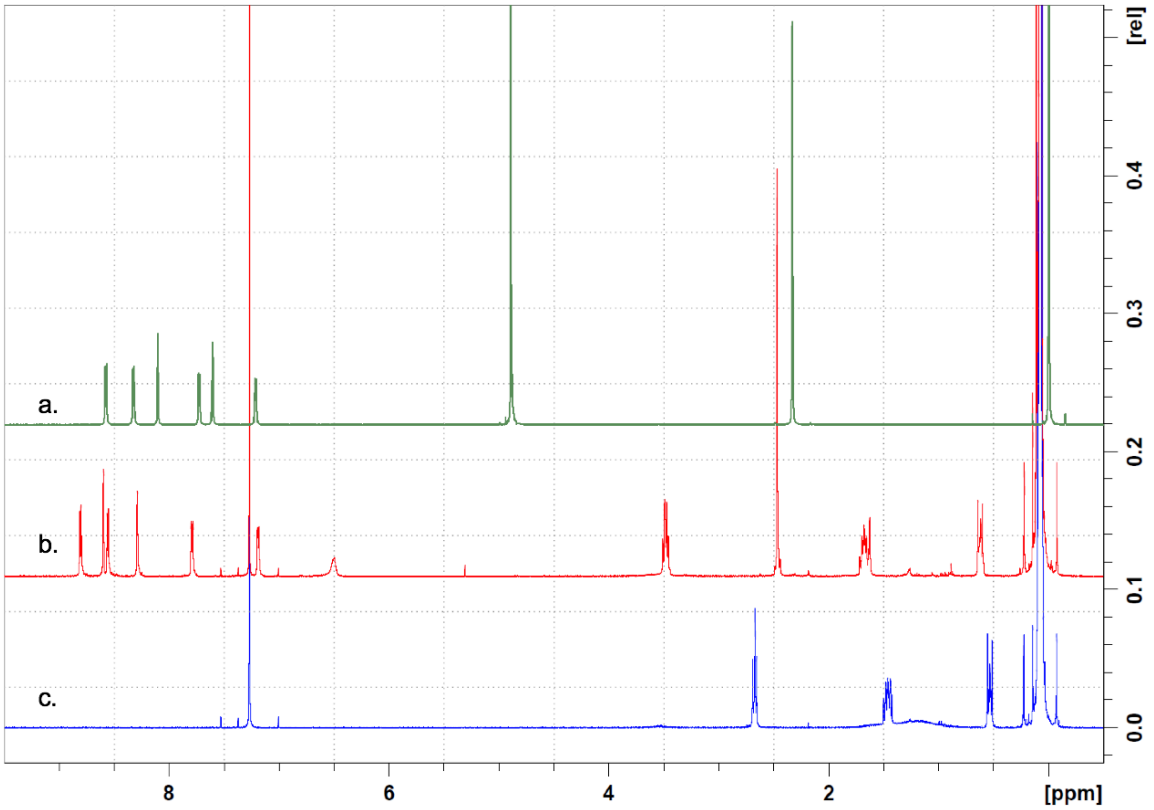

Figure 7: ^{1}H NMR spectra tracking the bpyPDMS synthesis a) mcbpy in D_2O/NaOD with TMS b) bpyPDMS in $CDCl_3$ c) NH_2PDMS in $CDCl_3$.

The triplet, multiplet, and triplet signals in the NH_2PDMS spectrum were characteristic of a propyl moiety ($CH_2CH_2CH_2$), and this was retained in the bpyPDMS spectrum as well as the six aromatic signals from mcbpy (δ 7-9 ppm). Additionally, the methyl peak in the mcbpy spectrum was retained in bpyPDMS at δ 2.4 ppm. The bpyPDMS analyzed contained relatively little impurities.

The molecular weights of 50 cSt NH_2PDMS determined by ^{1}H NMR spectroscopy are shown below in Table 1.

Table 1: Molecular weights of bpyPDMS determined by ^{1}H NMR.

NH_2PDMS Viscosity (cSt)	Molecular Weight (g/mol)	Molecular weight from manufacturer (g/mol)
50	2,970 (± 70)	3,000
100	5,400 (± 200)	5,000
1,000	20,000 (± 10,000)	25,000
5,000	41,000 (± 9,000)	50,000

The large uncertainties in the data indicated low precision within ^{1}H NMR spectra since the molecular weights were determined from the two CH_2 peaks. Regardless, the molecular weights given by the manufacturer were mostly within bounds of the calculated values. When plotting these molecular weights against their respective GPC retention times, there was good linearity (Figure 8).

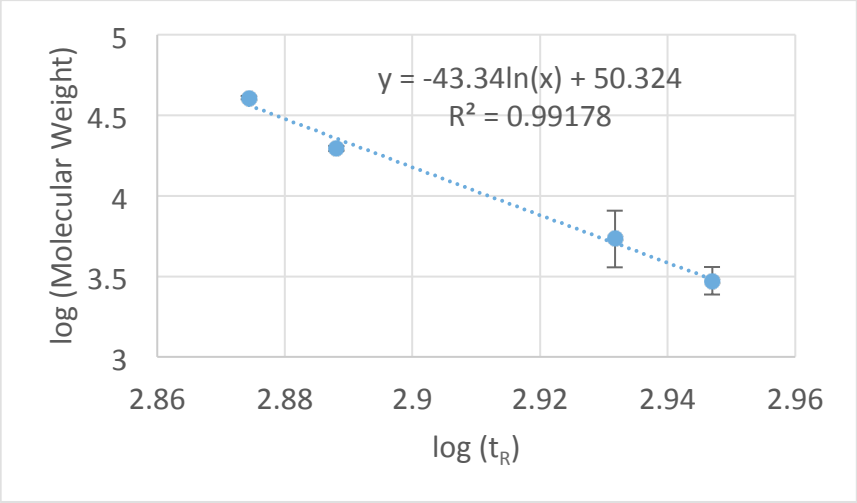

Figure 8: Precision of ^{1}H NMR molecular weights and GPC retention times for 50 cSt NH_2PDMS.

This relationship ensured that the sizes of NH_2PDMS polymer were separated effectively in the GPC column and that the ^{1}H NMR results coincided with other

instrumental methods. Determination of these molecular weights was essential in calculating the masses used in the formation of the cross-linked network and acted as verification for the manufacturer's values.

B. Gel-permeation chromatography (GPC)

Gel-permeation chromatography is a type of liquid chromatography in which large molecules are separated based only on size. The column consists of a stationary, solid matrix of styrene divinylbenzene (DVB), and detection is performed by UV-vis spectroscopy, which measures light absorbance and evaporative light-scattering. The ELSD operates by monitoring changes in a beam of light focused on a detector by solid non-volatile particles nebulized from the column. GPC allows for size and molecular weight differentiation of substances such as polymers. Larger molecules elute first while small molecules spend more time in the pores of the styrene DVB matrix.

As shown in Figure 9, a sample of 50 cSt bpyPDMS displayed UV absorbance at 295 nm while a sample of 50 cSt NH_2PDMS did not. This was due to the added bipyridine groups at the terminal ends of the PDMS chain. Moderate tailing was observed in this spectrum, suggesting that the composition of the mobile phase could have been improved. Tailing is attributed to the analyte spending too much time in the stationary phase, so a mobile phase with stronger eluent strength might be used. Figure 10 shows the ELSD chromatogram of these samples, and both curves overlayed onto each other. This indicated that each polymer was similar in molecular weight, and this was predicted since the masses of amine and bipyridine endgroups, though 151 g/mol apart, are insignificant compared to the mass of the PDMS backbone, which remained unchanged.

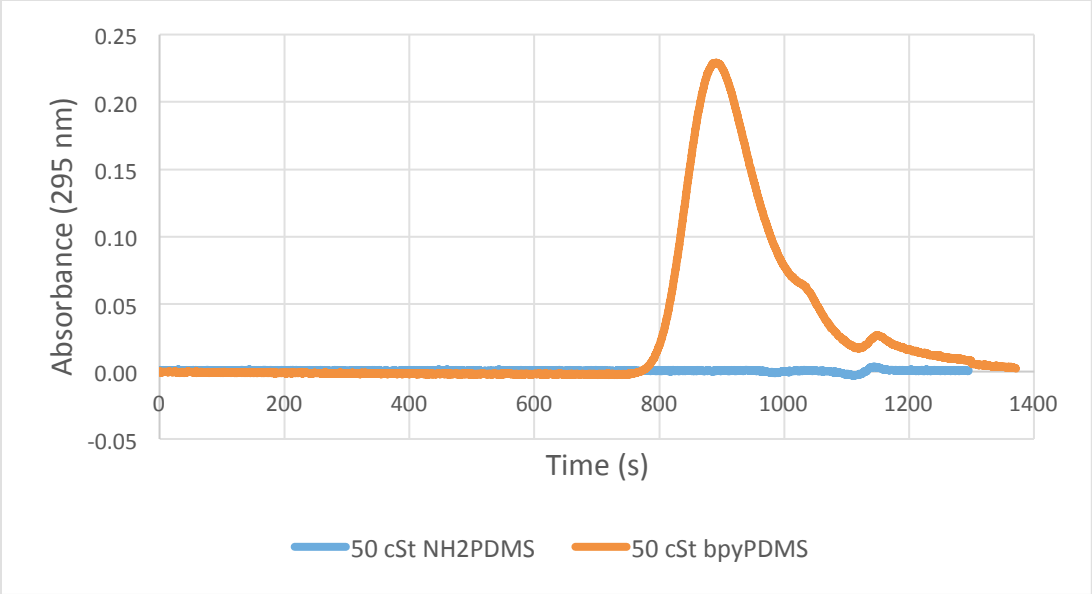

Figure 9: GPC UV chromatogram of NH_2PDMS and bpyPDMS taken at 295 nm in 3% n-butylamine: toluene.

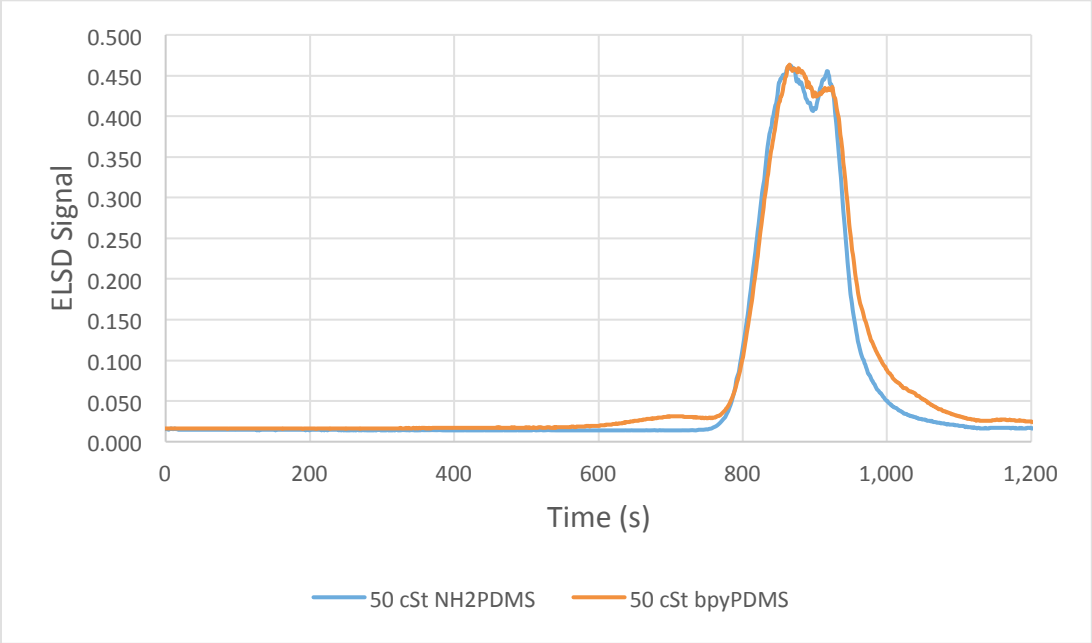

Figure 10: GPC ELSD chromatogram of NH_2PDMS and bpyPDMS in 3% n-butylamine: toluene.

The double peak shape in Figure 10 suggested the existence of two species with different molecular weights, and previous research showed the low molecular weight

peak was most likely cyclic PDMS.[12] The leftmost peaks were the bpyPDMS or NH_2PDMS signals since they had the highest molecular weight. In the process of synthesizing NH_2PDMS, octamethylcyclotetrasiloxane (D_4) is used in anionic and cationic ring-opening polymerization with an amine-terminated disiloxane, demonstrated in Figure 11, leaving cyclic species behind in the product mixture according to an equilibrium. These cyclic siloxanes have not been isolated and quantified, but may conflict with complexation and purity of the cross-linked polymer network.

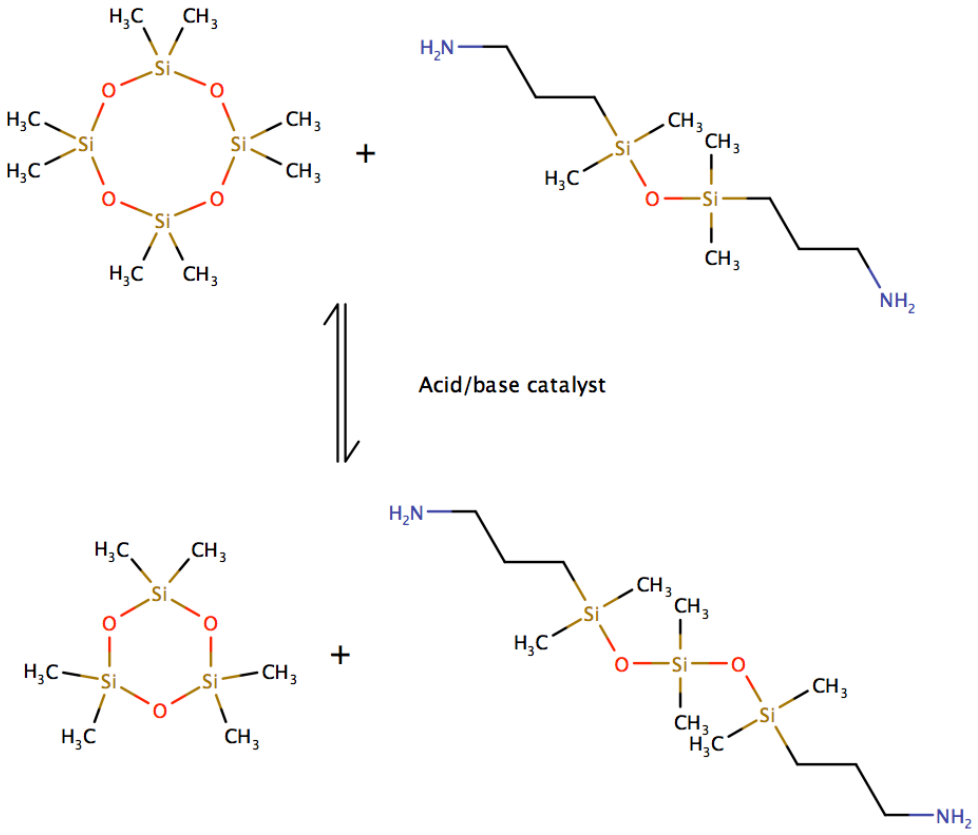

Figure 11: Polymerization in the synthesis of NH_2PDMS. One siloxyl group from the cyclic PDMS was incorporated into the chain in this example.[12]

Figure 12 below is a plot of ELSD signals from each molecular weight of bpyPDMS. The bpyPDMS signal seemed to decrease with molecular weight, but this was only due to inconsistent sample preparation. The bpyPDMS retention time decreased with molecular weight since higher molecular weight species exit the column first.

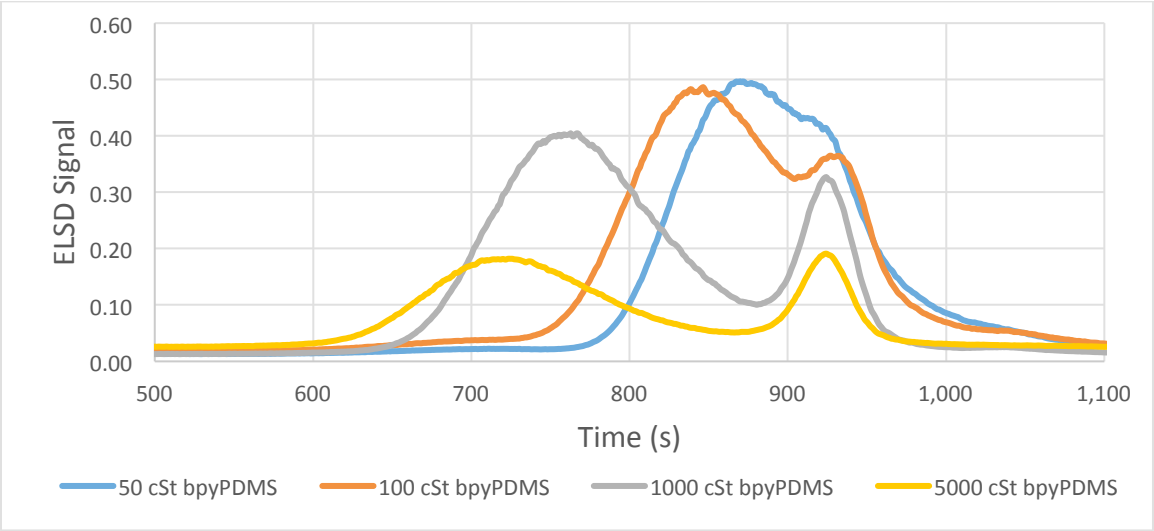

Figure 12: ELSD chromatograms of bpyPDMS samples.

Each molecular weight of bpyPDMS was resolved with characteristic retention times (5000 cSt, 722 s; 1000 cSt, 757 s; 100 cSt, 841 s; 50 cSt, 875 s). The retention time for the low molecular weight species did not vary from 927 s, suggesting its size was constant. The amount of this low molecular weight species seemed to increase with molecular weight, but this was not necessarily true between the 1000 cSt and 5000 cSt bpyPDMS samples. This would be better quantified by calculating the ratio of the bpyPDMS and low molecular weight peak areas, but there was not enough baseline resolution to do this.

When analyzing the corresponding UV-vis chromatograms for these bpyPDMS samples, absorbance at 296 nm by the low molecular weight species was observed

(Figure 13). This was not consistent with the structure of the cyclics proposed in Figure 12 since no species within these molecules was predicted to absorb at 295 nm.

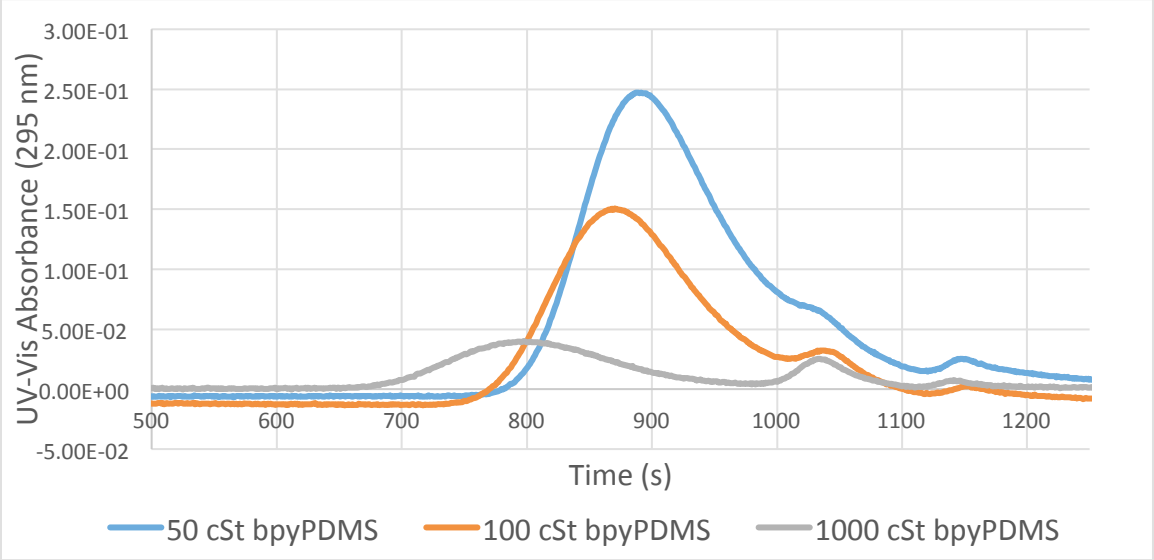

Figure 13: UV chromatograms of bpyPDMS samples.

Only three molecular weights of bpyPDMS are shown since the UV signal for the 5000 cSt bpyPDMS contained noise and did not display clear peaks, which was likely due to the smaller ratio of bipyridine: PDMS. The signal at 1029.5 s, which corresponded to the low molecular weight species, was shifted away from 927 s since the UV signal appeared to be slightly delayed from the ELSD. There were two low molecular weight signals in this chromatogram, which was inconsistent with Figure 13. The lowest molecular weight peak may have been due to unreacted mcbpy in the bpyPDMS synthesis, but the structure of the other low molecular weight species is still unknown. Either pieces of PDMS chain with bipyridine attached were being spliced or cyclic PDMS was reacting with bipyridine from mcbpy. It was even possible that there were

impurities present which also absorbed at 295 nm. Further experimentation is being conducted to answer this question.

Samples of 50 cSt and 5000 cSt NH_2PDMS were heated in an evacuated oven at 200^{o}C overnight in attempt to eliminate this low molecular weight species from the material through evaporation. The GPC chromatograms of heated NH_2PDMS and bpyPDMS made from this NH_2PDMS were compared to the unheated in Figure 14.

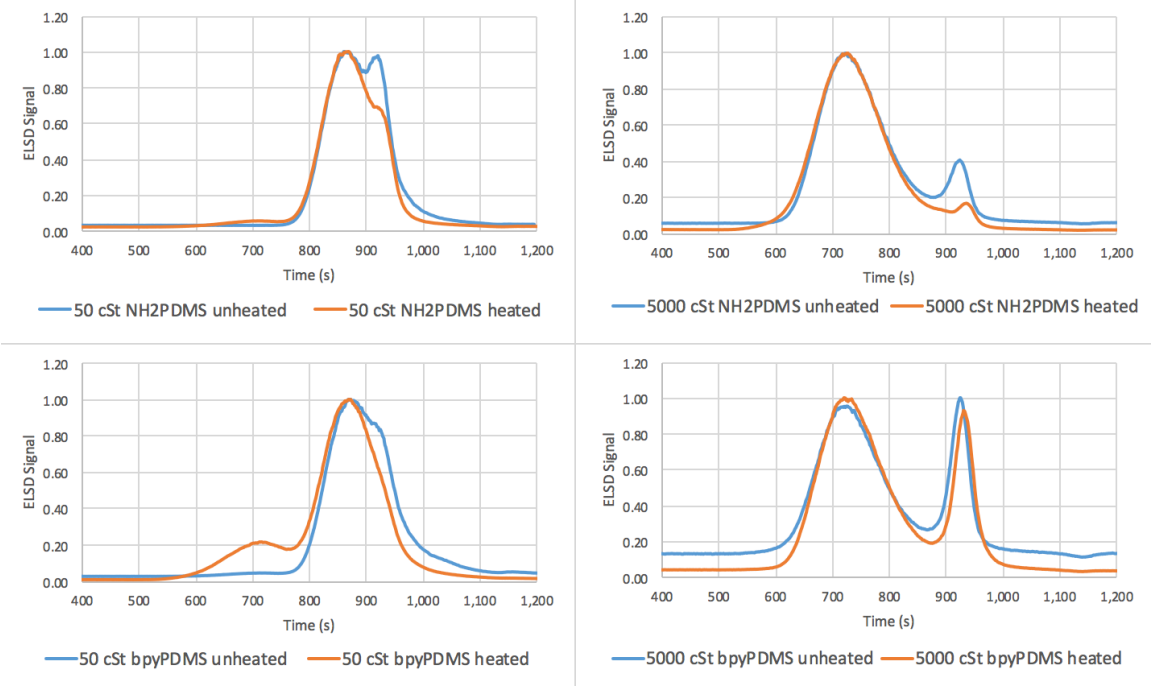

Figure 14: Comparison of heated and unheated samples of PDMS through ELSD chromatograms (normalized).

The low molecular weight peak decreased after the heat treatment in the NH_2PDMS samples, but not significantly in the bpyPDMS samples. The amount of low molecular weight material in bpyPDMS was mostly independent of the amount in NH_2PDMS. Since no difference was observed that would be useful, heat treatment was not used in synthesizing the network. When taking multiple chromatograms of each

sample, a high molecular weight peak would appear randomly. This was most likely residue leaching from the GPC column and had nothing to do with the sample itself.

C. Differential Scanning Calorimetry (DSC)

Differential scanning calorimetry is used to measure heat flow through a sample as a function of temperature, relative to a reference. This is useful in quantifying phase transitions, which include crystallization (exothermic), melting (endothermic), and glass transition temperatures (T_g). The quantity T_g is the temperature at which a polymer transitions from a hard, glassy phase to a soft, rubbery one. Samples are placed in crucibles, or small aluminum pans, then subjected to a temperature sequence. This usually involves cooling below the T_g, maintenance of this temperature for a few minutes to allow for equilibration then heating to a temperature above the melting point. The heat flow is measured in Joules, and exothermic (crystallization) peaks appear in the positive direction while endothermic (melting) peaks are in the negative direction for this analysis. This technique helps to identify thermodynamic properties of materials and understand their behavior.

DSC thermograms for samples of 50 cSt NH_2PDMS and bpyPDMS are shown below in Figure 15. The glass transition temperature is the leftmost peak, and for bpyPDMS, the crystallization peak is at -33.1 ^oC and the melting peak (endothermic) is at 48.0 ^oC. The area of each peak indicates the heat required to crystallize/melt the polymer per gram of sample. This comes from the units on the y-axis being W/g, so the integral of this unit with respect to time would be J/g.

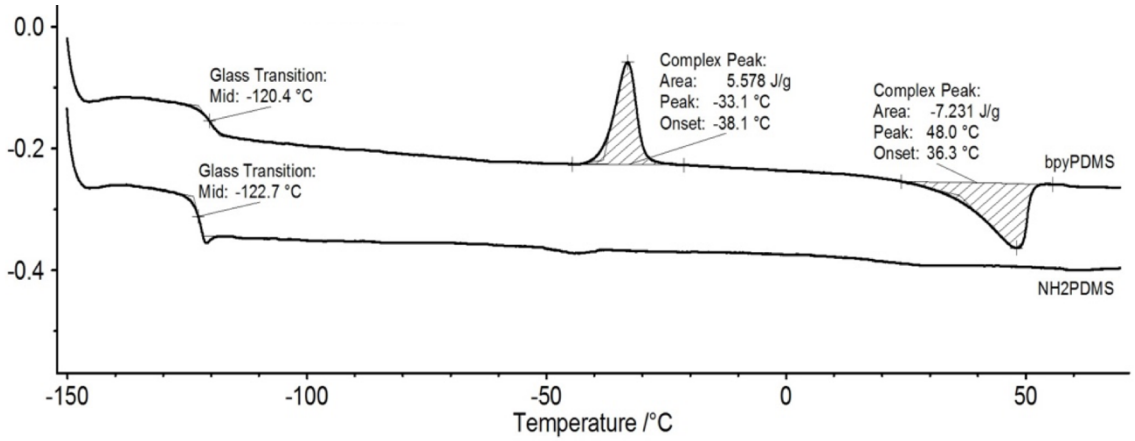

Figure 15: Comparison of DSC thermograms for 50 cSt NH_2PDMS and 50 cSt bpyPDMS.

Each sample displayed glass transitions of about -120 ^oC, and this was consistent with previous findings.[13] The bpyPDMS sample displayed significant crystallization and melting while NH_2PDMS did not, and this can be explained by the impact of endgroups (NH_2 or bipyridine) on the thermodynamic behavior.

Regular CH_3PDMS (linear PDMS) displays substantial crystallization and melting at a large range of molecular weights (at least 50 cSt to 5000 cSt) because individual PDMS chains are able to easily stack on one another. This is shown by the large crystallization and melting peak areas in 50 cSt CH_3PDMS, shown below in Figure 16.

Multiple heatings of the sample were used since the first heating is often misrepresentative of the actual thermodynamic behavior. These three heatings of CH_3PDMS showed good consistency between runs. In Figure 16 and subsequent thermograms, the plot from the second heating was used. Dollase, *et al.* observed two crystallization peaks at -98.5 ^oC and -47.4 ^oC and two melting peaks at -50.5 ^oC and

-34.0 °C for a sample of 16k CH_3-PDMS.[13] The results were similar for the 50 cSt CH_3PDMS below.

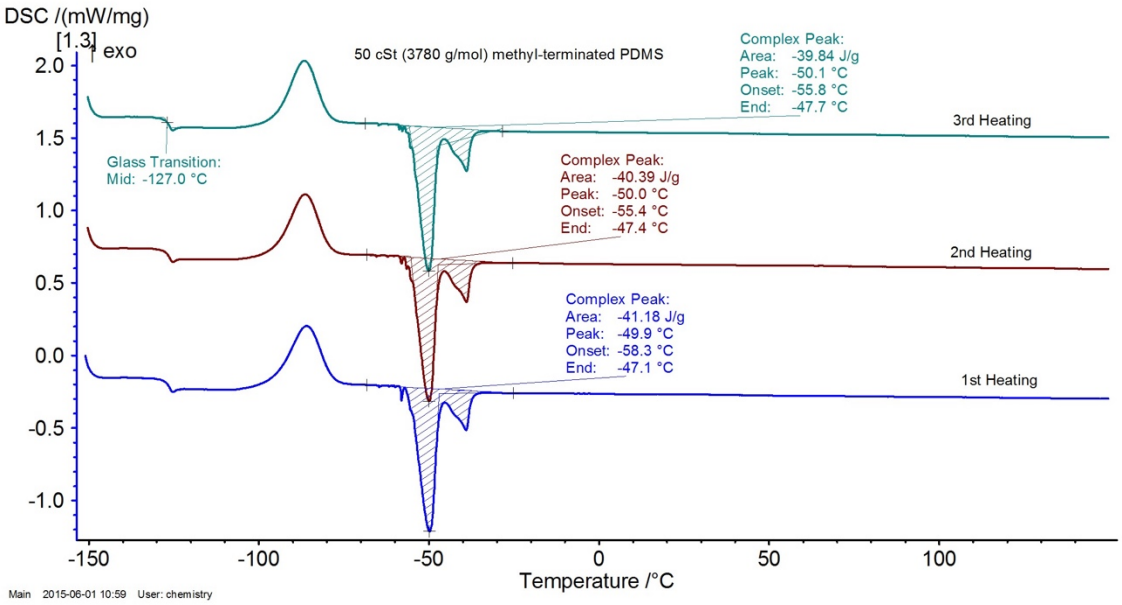

Figure 16: DSC thermogram of 50 cSt CH_3PDMS for three heatings.

In Figure 15, the % crystallinity, or abundance of crystals, for bpyPDMS was less than 50 cSt CH_3PDMS since the peak area was smaller (bpyPDMS 5.578 J/g, CH_3PDMS 25.43 J/g). The degree of crystallinity was further reduced in the NH_2PDMS sample since the peaks were practically non-present. This suggested that both bipyridine and NH_2 endgroups suppressed crystallization of PDMS chains. Aronson, et. al. predicted that, at high enough molecular weights, chains of NH_2PDMS could become long enough to display some PDMS crystallization even with this suppression, but this behavior was not observed with 50 cSt NH_2PDMS.[14] These results were also observed by Clarson, *et al.*[15]

The crystallization seen for bpyPDMS in Figure 15 couldn't have been from PDMS since crystallization occurred at a different temperature (-33.1 °C instead of

-85 ^{o}C). Torkelson, *et al.*, have shown that pyrene-terminated PDMS (crystallization -90.6 ^{o}C, melting -42.2 ^{o}C) displays 30% crystallization primarily because of the association of pyrene groups instead of the polymer backbone.[16] In this way, bipyridine groups were most likely crystallizing similarly to pyrene rings through π-π stacking, suppressing PDMS crystallization. The thermogram for NH_2PDMS appeared flat because amine groups do not crystallize as readily, and the amine groups suppressed most crystallization from PDMS.

The behavior of the iron (II) tris(bipyridine) PDMS network was investigated by DSC, and thermograms of bpyPDMS with $Fe(BF_4)_2 \cdot 6H_2O$ added in different proportions are shown below in Figure 17.

The green thermogram represents the fully cross-linked material with a bipyridine: iron (II) ratio of 3:1. These plots hardly resembled the one for plain bpyPDMS since the formation of $Fe(bpyPDMS)_3^{2+}$ disallowed bipyridine groups from crystallizing through π-π stacking and PDMS crystallization was suppressed, resulting in only melting transitions. Some bipyridine melting existed at 48.0 ^{o}C, but this signal decreased with increasing iron (II) as more bipyridine was being incorporated into the network. No crystallization was observed in these samples except for the one with excess iron (II), suggesting free iron (II) atoms were changing the thermodynamics of the cross-linked material.

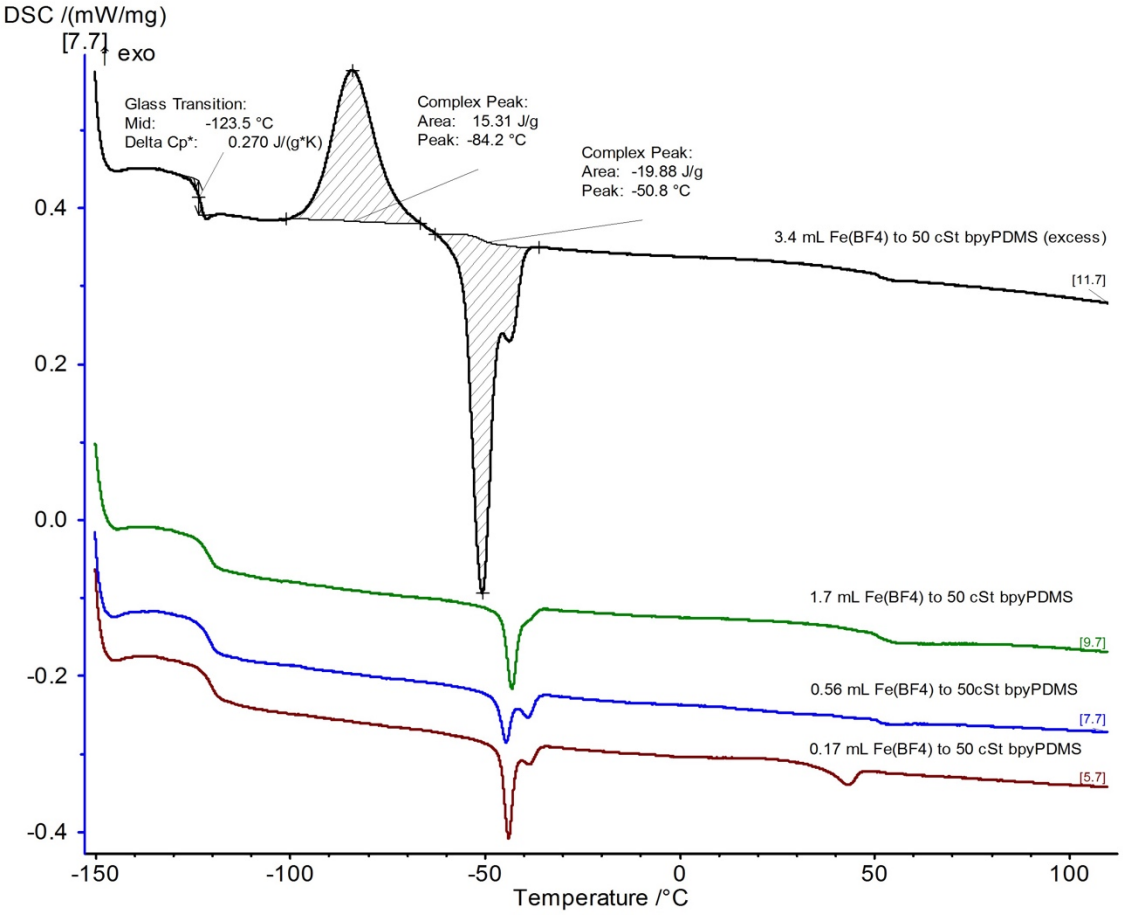

Figure 17: DSC thermograms of 50 cSt bpyPDMS with different ratios of $Fe(BF_4)_2 \cdot 6H_2O$ added. Burgundy = 77.7:1 bipyridine: iron (II), blue = 15.4:1, green = 2.64:1, black = 1.02:1.

The shape of the thermogram for bpyPDMS with excess iron (II) closely resembled that for CH_3PDMS, and this can be seen below in Figure 18.

The only way these two thermograms could have overlapped is if bipyridine groups were no longer contributing to the thermodynamic behavior of the network and became dissociated from PDMS chains. Otherwise, the thermogram would have looked like the one for bpyPDMS with a 3:1 ratio of bpy: iron (II). Also, as larger amounts of

iron (II) were added to this bpyPDMS sample, the thermogram converged even more towards CH_3PDMS, suggesting scission of PDMS chains increased with iron (II) concentration. The cutting of PDMS chains by free iron (II) atoms has not been previously documented, but this is currently the best explanation for this phenomenon. This issue will need to be resolved if complete networks of this material are to be formed without interferences. Beside this exception, the material behaved as predicted at ratios of bipyridine: iron (II) greater than or equal to 3:1.

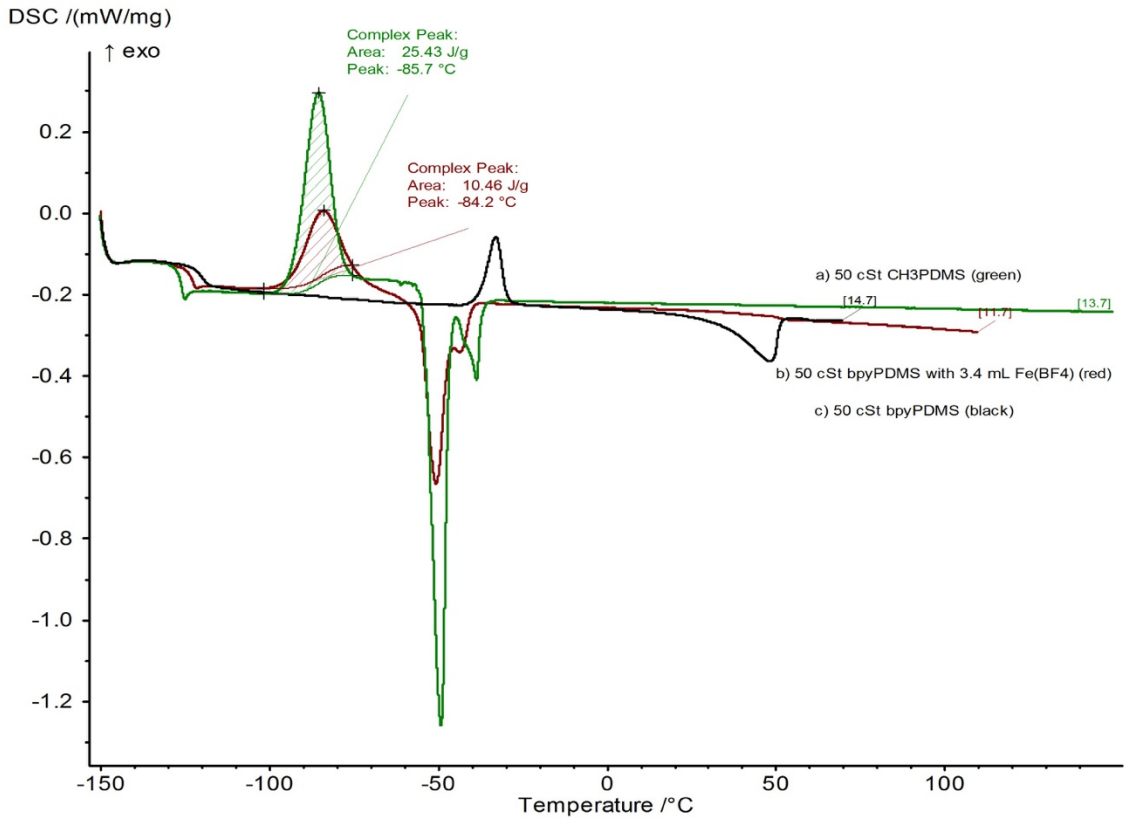

Figure 18: DSC thermograms of 50 cSt bpyPDMS (black line), 50 cSt bpyPDMS with $Fe(BF_4)_2 \cdot 6H_2O$ (red), and 50 cSt CH_3PDMS (green).

D) Cyclic voltammetry of the network

Cyclic voltammetry (CV) was performed on the iron (II) tris(bipyridine) PDMS network to determine whether an electric stimulus would reversibly oxidize the material in solution. The CV trace indicated a reversible, one-electron reduction/oxidation of the rubber film at a potential of 1.08 V versus SCE which was close to that seen for $Fe(bpy)_3(ClO_4)_2$ in acetonitrile (1.03 V).[17] As shown in Figure 19 below, the top peak indicates oxidation of the network to Fe^{3+} and bpyPDMS while the bottom indicates reduction to iron (II) tri(bipyridine) PDMS. The peak shape and peak-to-peak separation are consistent with a diffusion-controlled process, indicating that the electrode is able to contact iron centers relatively distant form the surface. This finding indicates some manner of charge migration through the material, which may be relevant to future applications as an electroresponsive rubber.

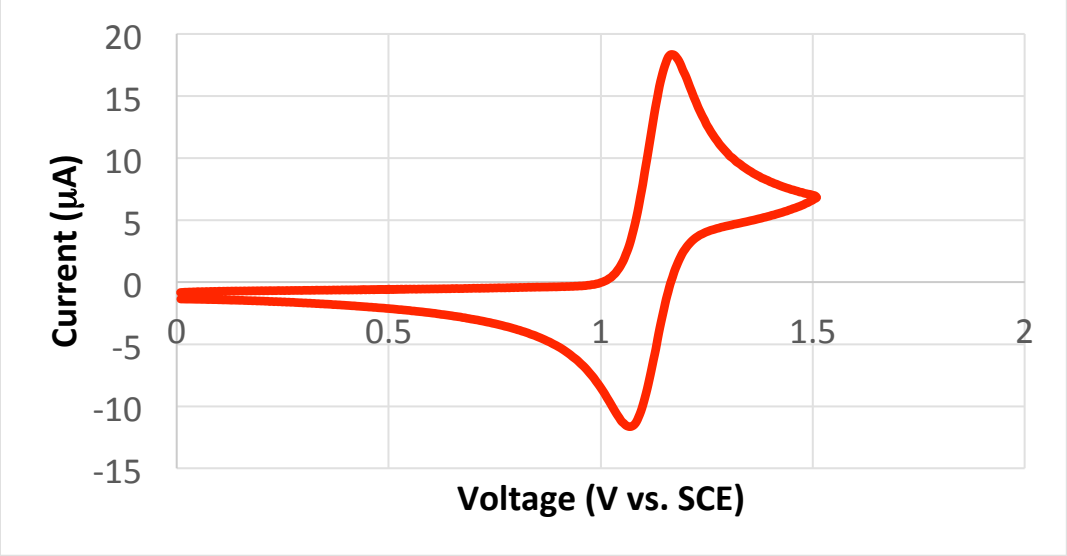

Figure 19: Cyclic voltammetry of the network.

The $Fe(bpy)_3$ complex was reversibly oxidized and reduced as predicted. This behavior introduces opportunities for electrode deposition, ease of processing, and recyclability since iron (II) tris(bipyridine) cross-links can be reversibly formed without hindering the potential for network formation. If the network was not able to form as readily after oxidation/reduction of the cross-links, the plot above would not be cyclic. In this way, changing the shape of the material in an industrial setting would be as easy as oxidizing the iron (II) cross-links, re-molding the resulting solution, and then reducing iron (III) to re-form the network.

E) Iron titrations of bpyPDMS samples

UV-vis spectroscopy was used to study the network formation of iron (II) tris(bipyridine) by monitoring its absorbance at 540 nm during additions of $Fe(BF_4)_2 \cdot 6H_2O$ or $FeCl_2 \cdot 4H_2O$ to bpyPDMS. This network formation is based on the following equilibrium:

$$Fe^{2+} + 3\ bpyPDMS \rightleftharpoons [Fe(bpyPDMS)_3)]^{2+} \qquad Equation\ 2$$

UV-vis spectra are obtained by scanning through a range of wavelengths selected by a monochromator and measuring the transmittance of light through a sample in comparison to a reference beam. The relationship between absorbance A and transmittance is:

$$A = -\log\left(\frac{I}{I_0}\right) \qquad Equation\ 3$$

The variables I and I_0 are the intensities of light exiting and entering the cuvette respectively. The absorbance is proportional to the concentration of iron (II) atoms in the cuvette according to Beer's law:

$$A = \varepsilon bc \qquad Equation\ 4$$

The variable ε is the extinction coefficient (constant property), b is the path length (width of cuvette, 1 cm), and c is the concentration of the absorbing species. The iron solution was made such that five 50 μL additions would result in a 3:1 ratio of bipyridine: iron (II) in the cuvette with an absorbance of 1. This was based on the extinction coefficient (ε = 9740 $M^{-1}cm^{-1}$ at λ_{max} = 540 nm) for $Fe(bpy)_3^{2+}$.

The series of spectra resulting from titrating 50 cSt bpyPDMS with a solution of $FeCl_2 \cdot 4H_2O$ are shown below in Figure 20.

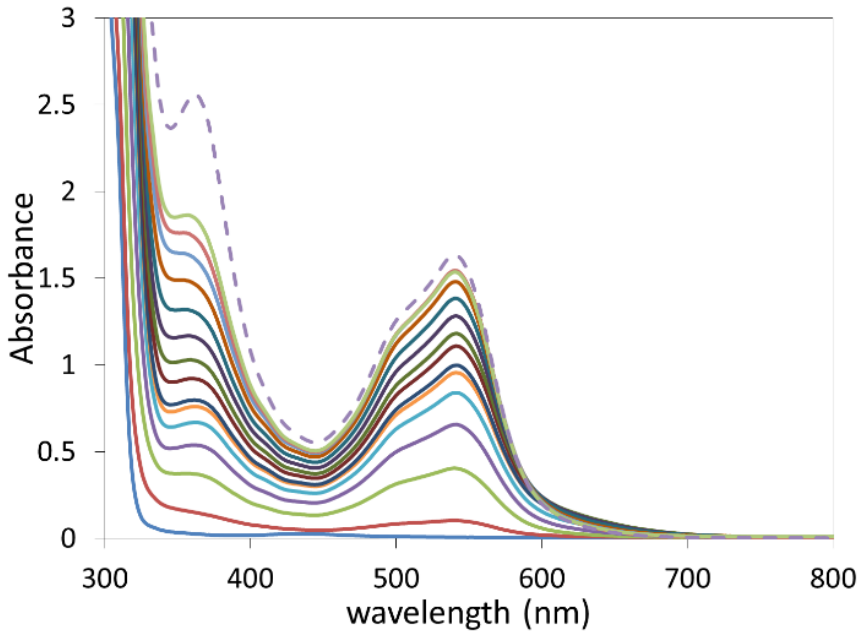

Figure 20: Series of UV-Vis spectra taken after additions of $FeCl_2 \cdot 4H_2O$ to bpyPDMS in THF.

The dotted line is a spectrum of the cuvette after 24 hours from the last addition. As iron was added to the cuvette, the absorbance at 540 nm increased and equilibrated at 1.5. This was called the endpoint, or where formation of the network neared completion and absorbance increased insignificantly for a given amount of iron (II). At the endpoint,

the ratio of bpy: iron (II) was found to be 0.94:1, which was different than the expected 3:1 ratio. Previous research has suggested that iron (II) may form complexes with chloride ions from $FeCl_2 \cdot 4H_2O$ that interfere with network formation.[18] These structures are shown below in Figure 21.

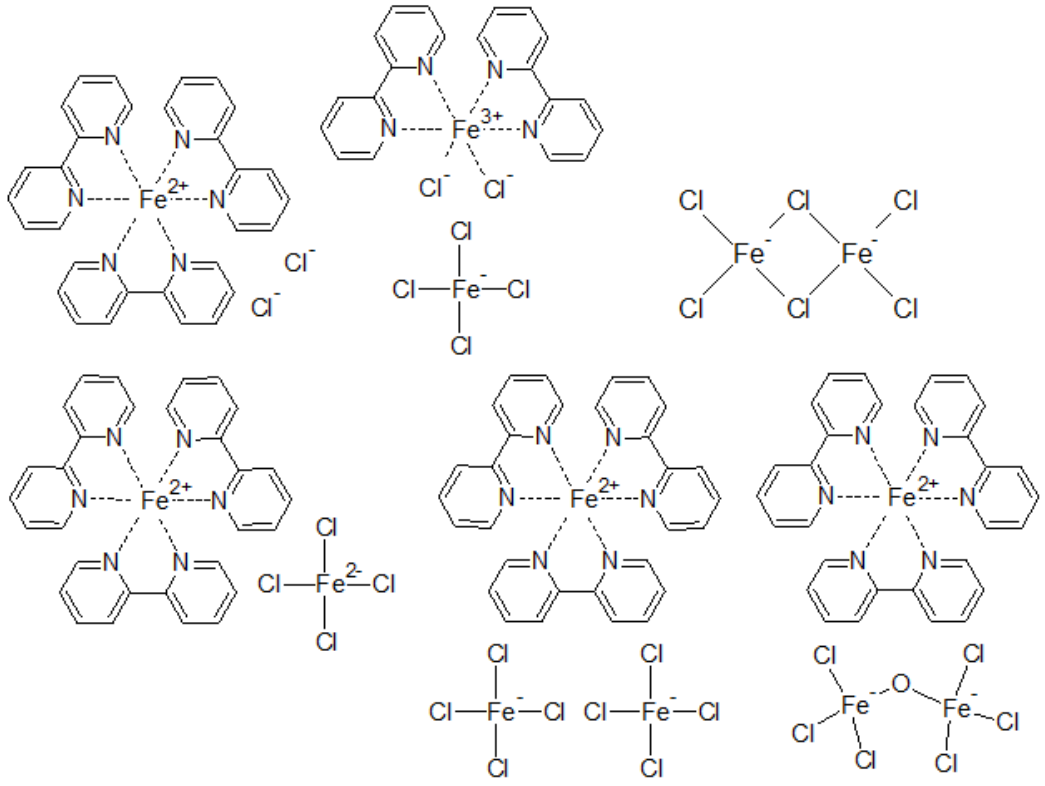

Figure 21: Possible complexes of iron (II), bpy, and chloride.

These undesired complexes absorb in the UV region at 360-375 nm, and absorbance at these wavelengths in the spectrum above was very pronounced (Figure 20). The extinction coefficients from each spectrum ($\varepsilon = \frac{A}{bc}$) were plotted versus the concentration of iron (II) in the cuvette. This was compared to the predicted curves for the following equilibria (Figure 22):

$$Fe^{2+} + 3\ bpy \rightleftharpoons [Fe(bpy)_3]^{2+} \qquad Equation\ 5$$

$$3\ FeCl_2 + 3\ bpy \rightleftharpoons [Fe(bpy)_3]^{2+} + Fe_2Cl_6^{2-} \qquad Equation\ 6$$

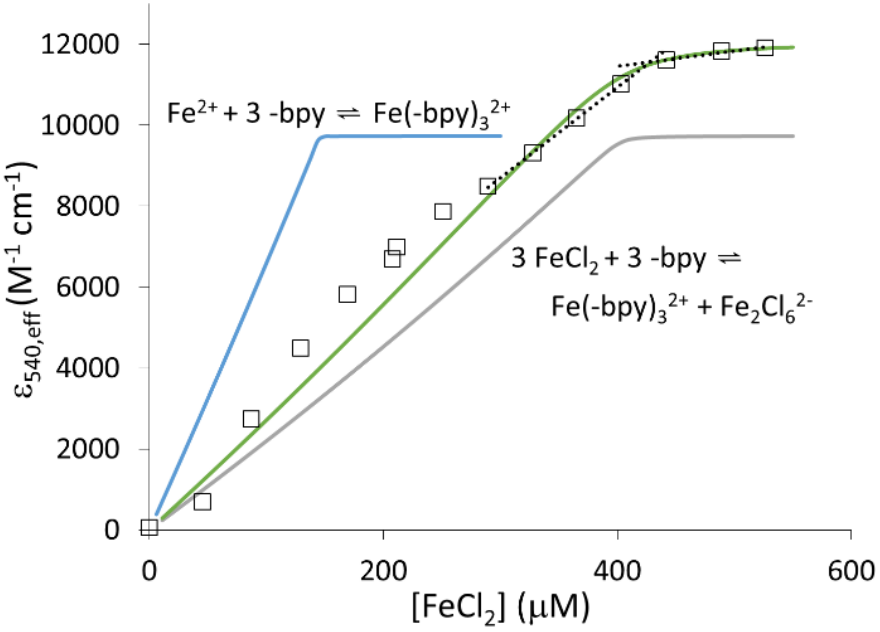

Figure 22: Plot of the extinction coefficients from titration spectra of $FeCl_2 \cdot 4H_2O$ and bpyPDMS versus $FeCl_2$ concentration in the cuvette with predicted curves (based on $\varepsilon = 9740\ M^{-1}cm^{-1}$).

The green line represents an approximate fit to the actual data acquired. The blue line represents bipyridine in a ratio of 3:1 bpy: iron (II) while the gray line represents a 1:1 ratio bpy: iron (II). Since the data existed between the curves for the two equilibria mentioned above, the sample was most likely a mixture of bipyridine complexes with iron (II) and chloride ions. Many structures of chloride complexes are possible, but these have not been determined. Ideally, the shape of this curve should follow the blue line, which represents full complexation of bpyPDMS and iron (II) atoms in a 3:1 fashion.

The results were improved for $Fe(BF_4)_2 \cdot 6H_2O$ since little absorbance was

observed at 360-375 nm and the calculated endpoint was the desired 2.9:1 bipyridine: iron (II) ratio. The series of spectra for these samples are shown below in Figure 23. The ratio of the absorbance peaks at 540 nm compared to 380 nm was greater than one in these spectra while the 380 nm peaks were slightly larger than the 540 peaks in Figure 20 because of the iron (II) chloride species.

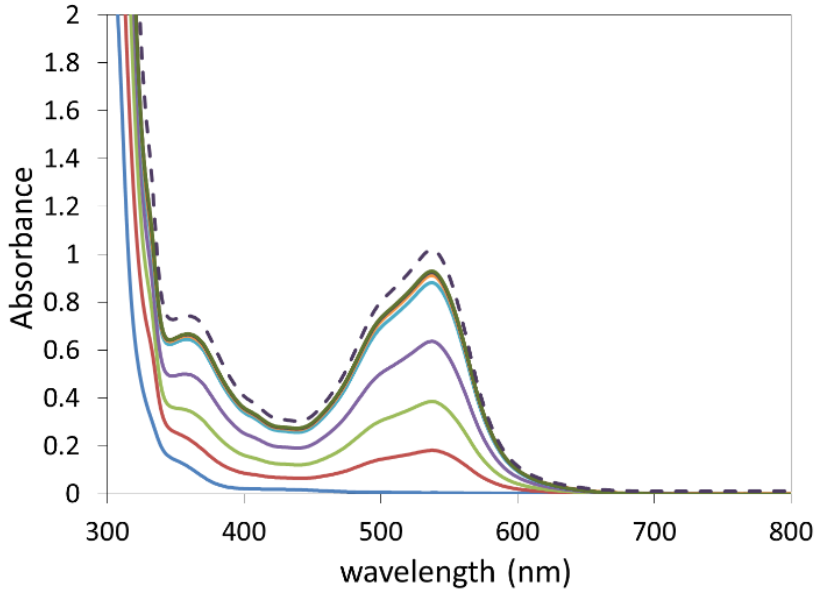

Figure 23: Spectra taken after titrations of bpyPDMS with $Fe(BF_4)_2 \cdot 6H_2O$ in THF.

The endpoint extinction coefficient was measured to be 8070 $M^{-1}cm^{-1}$, which implied a chelation efficiency, or percentage of network formation, of 0.83 when compared to the extinction coefficient for $Fe(bpy)_3^{2+}$ (9740 $M^{-1}cm^{-1}$). According to modern definitions, this is enough to be called a complete network.

F) Thin films of cross-linked network

Examples of sandwiches made from $FeCl_2 \cdot 4H_2O$ and bpyPDMS in MEK are shown below in Figure 24.

Figure 24: Film sandwiches of the iron (II) tris(bpy) PDMS material.

These films, though thin and transparent enough for UV-Vis analysis, were not able to be used since the iron (II) source was $FeCl_2 \cdot 4H_2O$, and it was not discovered until later that using this source resulted in networks with non-3:1 bpy: iron (II) ratios. Nevertheless, the figure above demonstrated that uniform films were able to be produced successfully.

Films made with $Fe(BF_4)_2 \cdot 6H_2O$ were much darker than those above since a larger proportion of bipyridine groups was complexed with iron (II) (3:1 ratio instead of 1:1). The film thickness would be have to be reduced to ~6 μm to make the material transparent enough, but this size cannot be achieved with the sandwich method. One alternate strategy is spin-coating, which allows for even distribution of polymer solutions and accurate control of the thickness of polymer films. It involves the introduction of a polymer solution onto a glass slide, then spinning the slide at a specific rpm until a film is produced. Preliminary results showed that films were too thin for analysis (< 1 μm). The specifications of this method are being optimized to achieve the correct film thickness.

G) Production of physical rubbery discs

Uniform physical discs of the cross-linked material were unable to be produced since the polymer solution used to deposit the material clung to the walls of the Teflon tube and could not be completely washed down with THF. Though the disc was not coin-

shaped as intended, it had red coloration and the texture was rubbery. The successful formation of a disc ~1 cm thick would be useful for measurements with dynamic mechanical analysis (DMA) or oscillating shear rheometry, which can help assess the quality of this material in comparison to other modern elastomers. Oscillating shear rheometers carry out stretches, bends, and twists in multiple directions to quantify the physical integrity of materials, and can be specialized to measure elasticity.

Conclusion:

The proposed iron (II) tris(bipyridine) PDMS material was able to be synthesized and characterized by multiple instrumental methods, and the network displayed unique properties. Though the molecular weights determined for NH_2PDMS contained significant uncertainty, accurate ratios of bipyridine: iron (II) were able to be replicated for synthesizing the network. Cyclic PDMS or low molecular weight species were detected in bpyPDMS samples, and these may have caused interferences in forming complete networks. Adding NH_2 endgroups, bipyridine endgroups, or iron (II) atoms suppressed PDMS crystallization, but with excess iron (II) the network thermogram resembled CH_3PDMS possibly due to chain scission. Using $FeCl_2 \cdot 4H_2O$ as the source of iron (II) introduced side complexes with chloride ions and prevented a 3:1 ratio of bipyridine: iron (II), but using $Fe(BF_4)_2 \cdot 6H_2O$ produced the correct ratios. Lastly, oxidation/reduction of the core $Fe(bpy)_3$ cross-links was able to be completed using cyclic voltammetry.

Future testing will involve forming thin films of the material for UV-vis analysis through methods such as spin-coating and subjecting physical discs of the network to oscillating shear rheometry. This will allow comparison of the elastic modulus for this

material to that of other rubbery products on the market. Additionally, the unique properties of iron (II) tris(bipyridine) PDMS networks will be further explored to elucidate the useful stimuli-responsive and recyclable properties of this new material.

References:

1. Abe, A. D., Karel; Kobayashi, Shiro, *Crosslinking in materials science: technical applications*. Springer Science & Business Media: 2005.

2. Gedde, U. W., *Polymer Physics*. Chapman & Hall: London, 1995; p 298.

3. Prabhu, R. K., Rasmus; Medvedev, Grigori A.; Caruthers, James M., A critical analysis of the effect of crosslinking on the linear viscoelastic behavior of styrene-butadiene rubber and other elastomers. *Journal of Polymer Science Part B: Polymer Physics* **2013,** *51* (8), 687-697.

4. Hotta, A.; Clarke, S. M.; Terentjev, E. M., Stress Relaxation in Transient Networks of Symmetric Triblock Styrene−Isoprene−Styrene Copolymer. *Macromolecules* **2001,** *35* (1), 271-277.

5. (a) Cordier, P. T., Francois; Soulie-Ziakovic, Corinne; Leibler, Ludwik, Self-healing and thermoreversible rubber from supramolecular assembly. *Nature* **2008,** *451* (7181), 977-980; (b) Sotta, P. F., C.; Demco, D.E.; Bluemich, B.; Spiess, H.W., Effect of residual dipolar interactions on the NMR relaxation in cross-linked elastomers. *Macromolecules* **1996,** *29* (19), 6222-6230.

6. Bokern, S. F., Ziyin; Mattheis, Claudia; Greiner, Andreas; Agarwal, Seema, Synthesis of new thermoplastic elastomers by silvr nanoparticles as cross-linker.

Macromolecules **2011,** *44* (12), 5036-5042.

7. Belfiore, L. A.; McCurdie, M. P.; Ueda, E., Polymeric Coordination Complexes Based on Cobalt, Nickel, and Ruthenium That Exhibit Synergistic Thermal Properties. *Macromolecules* **1993,** *26* (25), 6908-6917.

8. Appel, E. A. d. B., Jesus; Loh, Xian Jun; Scherman, Oren A., Supramolecular polymeric hydrogels. *Chemical Society Reviews* **2012,** *41* (18), 6195-6214.

9. (a) Burnworth, M. R., Stuart J.; Weder, Christoph, Structure-property relationships in metallosupramolecular poly(p-xylylene)s. *Macromolecules* **2012,** *45* (1), 126-132; (b) Kumpfer, J. R.; Wie, J. J.; Swanson, J. P.; Beyer, F. L.; Mackay, M. E.; Rowan, S. J., Influence of Metal Ion and Polymer Core on the Melt Rheology of Metallosupramolecular Films. *Macromolecules* **2011,** *45* (1), 473-480.

10. McCafferty, D. G.; Bishop, B. M.; Wall, C. G.; Hughes, S. G.; Mecklenberg, S. L.; Meyer, T. J.; Erickson, B. W., Synthesis of Redox Derivatives of Lysine and Their Use in Solid-Phase Synthesis of a Light-Harvesting Peptide. *Tetrahedron* **1995,** *51* (4), 1093-1106.

11. Noviandri, I. B., K.; Fleming, D.; Gulyas, P.; Lay, P.; Masters, A.; Phillips, L., The decamethylferrocenium/decamethylferrocene redox couple: a superior redox standard to the ferrocenium/ferrocene redox couple for studying solvent effects on the thermodynamics of electron transfer. *J. Phys. Chem. B* **1999,** *103*, 6713-6722.

12. Yilgor, I. M., James E., Polysiloxane-containing copolymers: a survey of recent developments. *Advances in Polymer Science* **1988,** *86*, 1-86.

13. Dollase, T.; Spiess, H. W.; Gottlieb, M.; Yerushalmi-Rozen, R., Crystallization of PDMS: The effect of physical and chemical crosslinks. *EPL (Europhysics Letters)* **2002,** *60* (3), 390.

14. Roland, C. M.; Aronson, C. A., Crystallization of polydimethylsiloxane end-linked networks. *Polymer Bulletin* **2000,** *45* (4-5), 439-445.

15. Clarson, S. J. D., K.; Semlyen, J. A., Studies of cyclic and linear poly(dimethylsiloxanes): 19. Glass transition temperatures and crystallization behavior. *Polymer* **1984,** *26*, 930-934.

16. Jones, B. A.; Torkelson, J. M., Crystallization and Enthalpy Relaxation of Physically Associating, End-Linked Polymer Networks: Telechelic Pyrene-Labeled Polydimethylsiloxane. *Polymer Bulletin* **2004,** *51* (5-6), 411-418.

17. Saji, T.; Aoyagui, S., Polarographic studies on bipyridine complexes: I. Correlation between reduction potentials of iron(II), ruthenium(II) and osmium(II) complexes and those of free ligands. *Journal of Electroanalytical Chemistry and Interfacial Electrochemistry* **1975,** *58* (2), 401-410.

18. (a) Ariyananda, L. M. D.; Norman, R. E., Tris(2,2'-bipyridyl-N,N')iron(II) bis[tetrachloroferrate(III)]. *Acta Crystallographica E* **2002,** *E58*, m775-m776; (b) Figgis, B. N.; Reynolds, P. A., cis-Bis(bipyridyl)dichloroiorn(III) Tetrachloroferrate(III), $[Fe(bpy)_2Cl_2][FeCl_4]$; Structure at 4.2 and at 115 K by Neutron Diffraction. *Acta Crystallographica B* **1983,** *39*, 711-717; (c) Eckenhoff, W. T.; Biernesser, A. B.; Pintauer, T., Structural characterization and investigation of iron(III) complexes with

nitrogen and phosphorus based ligands in atom transfer radical addition. *Inorganica Chimica Acta* **2012,** *382*, 84-95; (d) Witten, E. H.; Reiff, W. M.; Lázár, K.; Sullifan, B. W.; Foxman, B. M., The Ferric Chloride-a-Diamine System. 3. X-ray Crystallographic, Magnetic Susceptibility, And Zero- and High-Field Mössbauer Spectroscopy Investigation of $[Fe(2,2'\text{-bpy})_2Cl_2][FeCl_4]$: Slow Paramagnetic Relaxation and Magnetic Ordering of Complex Bimetallic Salts. *Inorganic Chemistry* **1985,** *24*, 4585-4591; (e) Haselhorst, G.; Wieghardt, K.; Keller, S.; Schrader, B., The (m-Oxo)bis[trichloroferrate(III)] Dianion Revisited. *Inorganic Chemistry* **1993,** *32*, 520-525; (f) Weiss, H.; Strähle, J., Synthese und Kristallstruktur von Tris(2,2'-bipyriein)eisen(II) mOxo-bis(trichloroeisen(III)), ein Salz mit dem Anion $Fe_2OCl_6^{2-}$. *Zeitschrift für Naturforschung B* **1984,** *39b*, 1453-1455.

Vita:

Jacob Tyler Pawlik was born in Hickory, North Carolina on September 17, 1994 to James and Rhonda Pawlik. He graduated *Summa Cum Laude* from Appalachian State University with University and Deparmental Honors in May 2016. He achieved a Bachelor's of Science in Certified Chemistry with a Minor in Mathematics.

Jacob was involved in the NSF-STEP Program at Appalachian from 2013-2014 and participated in the National Conference for Undergraduate Research in Spokane, Washington in 2015. He was also involved in an off-campus biochemical industry in Boone called Molecular Toxicology, Inc. and did some previous work with Marlin Company, Inc. in Lenoir, North Carolina. Outside of chemistry, Jacob was on the Student Leadership Team at the Appalachian Wesley Foundation and participated in many student ministry events.

In the Fall of 2016, Jacob plans to pursue a P.h.D. in Chemistry from the University of North Carolina-Chapel Hill. After completing this degree program, he hopes to enter an industrial research position for a few years then become a full-time professor at a university.